DISTRIBUTION STATEMENT A. Approved for public release. Distribution is unlimited.

16th World Congress in Computational Mechanics (WCCM)
21-26 July 2024, Vancouver, Canada
A. Korobenko, M. Laforet, S. Prudhomme, R. Vaziri (Eds)

EFFECT OF LONG-TERM SEA WATER EXPOSURE VIA ACCELERATED LIFE TESTING ON DIELECTRIC MATERIALS

EUGENIA L. STANISAUSKIS WEISS[1], EMILY L. GUZAS[1]

[1] Naval Undersea Warfare Center (Division Newport)
1176 Howell St
Newport, RI 02841

Key words: Dielectric Materials, Sea Water Exposure, Material Aging.

Abstract. Dielectric materials, which are commonly used in capacitors, could increase energy storage density on a per volume basis in film capacitors compared to current technologies accommodating ever-increasing power demands. Recent work in this area has brought about dramatic increases in the dielectric permittivity and moderate increases in dielectric loss, leading to increased material performance on a per volume basis. However, little is known about the aging and breakdown of these materials, which could decrease the performance of these films over time due to decaying dielectric loss and energy storage density. A basic study of the aging of two different state-of-the-art dielectric materials, 3M's Very High Bond (VHB) 4910, commonly used in actuator applications, and bi-axially oriented polypropylene (BOPP), commonly used in large wound film capacitators, is completed. Accelerated life tests using distilled water are conducted to simulate the aging of these materials in a marine environment. An acceleration factor is determined by diffusion studies of distilled water into the materials. Aminabhavi's and Crank's methods are used and compared to compute the diffusion coefficient. The two methods produce identical activation energies and, in turn, acceleration factors. The success of this work could actively exhibit the promise of these materials in microelectronic uses.

1 INTRODUCTION

Dielectric elastomers and films are part of a broad range of materials commonly used in adaptive structures due to their unique capabilities for real time control of a structure's shape, stiffness, and damping [7, 21, 22, 23]. Other application areas include robotics [14, 19, 20], optical switches and speakers [9, 17], and prosthetic power capacitors [16, 23, 24]. These materials provide a unique combination of being able to withstand large

DISTRIBUTION STATEMENT A. Approved for public release. Distribution is unlimited.

deformation while being lightweight. Furthermore, the shape of these materials can be controlled by varying the application of electric field across the material. These materials can also be used in polymer-based wound film dielectric capacitors, which provide a scalable and cost-effective energy storage approach, designable with predictable failure modes. However, little work has been done to study the aging of these materials when exposed to an underwater environment over long periods of time. An evaluation of the aging and breakdown of dielectric materials is necessary so that future measures can be taken to prevent or delay material breakdown or failure.

The major physical and environmental mechanisms leading to degradation of an elastomer's nominal thermo-electro-mechanical properties include impact damage, mechanical fatigue, humidity, and fluid exposure. Types of degradation include: oxidation, photo-oxidation, thermal and thermo-oxidation, ozone-induced, mechanical, chemical, and hydrolytic. In an underwater environment, materials are most likely to undergo hydrolytic degradation due to long-term immersion in salt water. Previous work studying the effects of salt vs distilled water found the salt water to degrade the material properties to a similar or lesser degree than distilled water. This work will study the aging of two different dielectric elastomers via accelerated life tests using distilled water to determine how the materials change over time when exposed to an underwater environment. This will allow for the production of aged specimens for further testing, modeling, and analysis. The success of this work could actively exhibit the promise of these materials in microelectronic uses.

Two state-of-the-art dielectric elastomer materials are chosen for the current study. The first material, Very High Bond (VHB) 4910 from 3M (St. Paul, MN), is commonly used in actuator applications. The second material, bi-axially oriented polypropylene (BOPP), is commonly used in large wound film capacitators. Both of these materials present various advantages as dielectric materials. Aside from being commercially available, these materials support a high dielectric breakdown strength and contain the ability to sustain high electric fields, making these materials good candidates for sustained insulating performance. The limitation of BOPP lies in its low energy storage density and VHB's is in its high pre-strain, which are both active areas of research. The focus of this work will center on a basic study of the aging of these dielectric materials.

The paper is organized as follows: in Section 2, the experimental protocol of the accelerated life testing is discussed along with details about the materials studied. Section 3 describes the material conditioning method in detail. Results obtained via the accelerated life testing are presented and discussed in Section 4. The paper is closed by a few concluding remarks.

2 EXPERIMENTAL PROTOCOL

Experimental protocols described herein involve the selection and design of experimental specimens of the chosen materials, aging of these specimens, and mechanical testing of unaged and aged specimens to quantify any degradation in select viscoelastic properties. Experiments are divided into the main categories of specimen conditioning and characterization of mechanical properties.

2.1 Materials

Two different commercially available dielectric elastomer materials are studied: VHB4910 from 3M (St. Paul, MN) and BOPP. VHB4910 is an acrylic elastomer characterized by an operating temperature range of -10 to $90℃$ and a low mass density of $0.96 g/cm^3$[1]. BOPP is a dielectric thin film with a mass density of $0.91 g/cm^3$ and an operating temperature range of 0 to $105℃$. BOPP possesses an oriented semi-crystalline morphology, which provides a high dielectric breakdown strength in the preferred direction. Both materials provide their own challenges originating from their unique characteristics, e.g. VHB's sticky surface in combination with its soft behavior, and BOPP's transparency combined with its manufacturing restriction to very thin films, with a maximum thickness of $0.05 mm$.

Specimens intended for post-aging tensile testing are cut from bulk material according to ASTM standards. Specimen sizing for VHB was per ASTM D638 [5] and BOPP specimens dimensions follow ASTM D882-18 [6]. The nominal thickness of $1 mm$ and non-rigidity of VHB4910 classify the test specimens as Type IV. A Type IV die is used to cut the VHB into specimens with a narrow width of $6 mm$, narrow length of $33 mm$, overall width of $19 mm$, overall length of $115 mm$, and gage length of $25 mm$. All dimensions are confirmed with the use of either a micrometer or ruler. The plastic backing covering the cut VHB specimens is removed prior to submersion and testing. The nominal thickness of BOPP is $0.05 mm$. Specimens are cut by hand to a width of $13 mm$ with a maximum variance of $0.3 mm$ over 4 width measurements per specimen. The lengths of the specimens are predetermined by the size of the initial sheet ($216 mm \; x \; 280 mm$). Due to the anisotropy of the material, two types of specimens are created, one parallel to the long edge and one parallel to the short edge of the sheets, to study the potential effect of anisotropy. A total of 135 specimens are cut (45 VHB, 45 BOPP-long, 45 BOPP-short).

2.2 Accelerated life testing setup

The aging process consists of immersion in water baths per a prescribed temperature protocol to achieve accelerated aging of the specimens. The aging setup consists of multiple acrylic plastic containers placed in either lab convection ovens or on a laboratory bench depending on the assumed operating temperature for in-service conditions. An illustration of the experimental setup can be seen in Figure 1. The plastic containers are filled with distilled water and contain the submerged specimens. Previous work by Heshmati et al. concluded that salt water degrades the mechanical properties of adhesives to a lesser degree than distilled water [13]. The use of distilled water (1) simplifies the challenge of maintaining salinity throughout the entire aging process and (2) provides a more conservative estimate of the aging process. A similar trend is also observed in Rudawka et al. even though salt water was compared to tap water [15]. Despite the stickiness of VHB, the specimens are able to remain submerged without assistance. The specimens, however, are placed on a bed of marbles to prevent adhesion of the specimens to the tank over time. The size of the positively buoyant BOPP specimens poses a challenge for long-term submersion. Stainless steel metal rods are placed on top of the BOPP specimens to maintain a submerged condition. All

specimens, regardless of material, are laid on a bed of marbles to allow for penetration of the water on both sides of the material. Two ovens (Cale-Parmer Stable Temp SN.W125419 SKU.52412-85 and Precision Oven Model 45EM SN.601111258 Cat.51221135) were used to maintain a constant elevated temperature to accelerate the exposure. Thermocouples (Omega DP80 Series SN.92032468 ID.27952 PA.6604346293) are used to monitor the temperature of the ovens to ensure stability. A temperature of 65°C is utilized for an elevated acceleration factor, as this is the highest temperature the plastic tanks can tolerate without deteriorating. Specimens are exposed at this temperature for a maximum of 128 days. This is a sufficiently long period to simulate either twelve or six months of real-time exposure in the assumed in-service environment. Distilled water is regularly added to the plastic containers to ensure water levels submerge the samples completely.

3 MATERIAL CONDITIONING

A diffusion study is carried out at three temperatures (23℃, 45℃, 65℃) to determine the effect of temperature on distilled water ingression into the specimens using two different methods [2, 11]. This diffusion data, coupled with Arrhenius' methodology, allows for the calculation of an acceleration factor relating laboratory exposure time at elevated temperature to real-life service time.

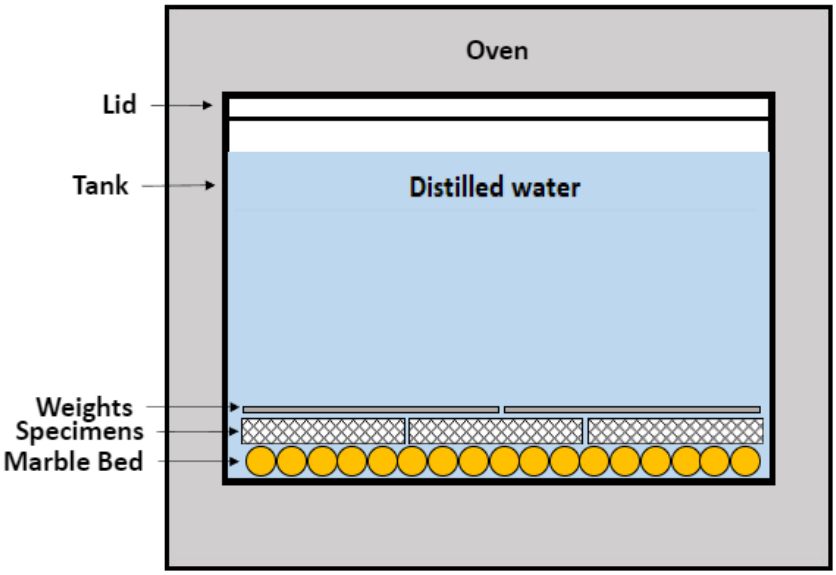

Figure 1: Illustration of accelerated aging experimental setup

3.1 Determination of the acceleration factor

Prior to conditioning the specimens, the acceleration factor (AF) must be determined. This acceleration factor is a constant ratio of the time spent in accelerated aging, t_{acc}, to its corresponding simulated time in the real-life service environment, t_{real}.

$$AF = \frac{t_{real}}{t_{acc}} \quad (1)$$

The determination of the acceleration factor is based on calculations of the activation energy necessary to complete the diffusion of the solution into the material at the various temperatures tested [10, 20]. Specimens are immersed in a distilled water bath at different temperatures. Their masses are periodically measured to track any changes in mass due to water uptake as per ASTM D570-98 [4]. The water uptake is observed to be Fickian and can, therefore, be modeled using Fick's second law of diffusion in 1D

$$\frac{dC}{dt} = D\frac{d^2C}{dx^2} \tag{2}$$

where C is the water concentration, D is the diffusion coefficient of the solution into the material, t is time, and x is the position in the sample. Assumptions that the specimens are initially free of moisture, the initial concentration distribution is uniform, temperature is constant, fluid pressure is constant, surface concentrations are equal, and the diffusion coefficient is constant are applied to Equation 2. This reduces Fick's second law of diffusion to

$$\frac{M_t}{M_\infty} = 1 - \frac{8}{\pi^2}\sum_{n=0}^{\infty}\frac{1}{(2n+1)^2}e^{\left[-\frac{D(2n+1)^2\pi^2 t}{4l^2}\right]} \tag{3}$$

where M_t is the total diffusion substance absorbed by the plate at time t, M_∞ is the quantity of diffusion substance gained after an infinite time (saturation), D is the diffusion coefficient, and l is the thickness of the specimen [11].

Two different methods, Aminabhavi's method [2] and Crank's method [11], can then be used to calculate the diffusion coefficient from Equation 3. Aminabhavi's method proposes that given changes in mass below 60% of the equilibrium value, Equation 3 can be approximated to

$$\frac{M_t}{M_\infty} = \frac{4}{l}\left(\frac{D}{\pi}\right)^{\frac{1}{2}} t^{\frac{1}{2}}. \tag{4}$$

The diffusion coefficient can be determined from the slope of the linear portion of a normalized mass change vs square root of time plot from Equation 4. The second method, Crank's method, calculates the diffusion coefficient at the time at which half of the equilibrium diffusion substance has penetrated the substance, $\frac{M_t}{M_\infty}\left(t = t_{\frac{1}{2}}\right) = 0.5$,

$$D = \frac{0.049l^2}{t_{\frac{1}{2}}}. \tag{5}$$

With estimates of the diffusion coefficient in hand, the temperature dependence of the diffusion coefficient can now be modeled using Arrhenius' equation, which governs the rate of the reaction as a function of temperature [3]. The Arrhenius equation can be written as follows:

$$D = D_0 e^{-\frac{E_a}{RT}} \tag{6}$$

$$\ln(D) = \ln(D_0) - \frac{E_a}{RT} \tag{7}$$

where D is the diffusion coefficient, D_0 is the pre-exponential factor, E_a is the activation energy, R is the ideal gas constant, and T is the absolute temperature of the diffusing substance. Obtaining the slope of a $\ln(D)$ vs $\frac{1}{T}$ plot gives the activation energy.

The acceleration factor can then be determined with

$$AF = \frac{D_a}{D_w} = \frac{D_0 e^{-\frac{E_a}{RT_a}}}{D_0 e^{-\frac{E_a}{RT_w}}} = e^{\frac{E_a}{R}\left(\frac{1}{T_w} - \frac{1}{T_a}\right)} \tag{8}$$

where D_a is the diffusion coefficient for the accelerated laboratory testing at temperature T_a and D_w is the diffusion coefficient at the service temperature T_w.

4 RESULTS AND DISCUSSION

The normalized sample weight vs time is measured to obtain a plot of the Fickian diffusion behavior where the water uptake steadily increases over time until an equilibrium point is reached upon which a steady value is maintained. The data are then be plotted as normalized mass change vs the square root of time for each temperature as seen in Figure 2 and modeled using Equation 4. The water diffusion kinetics is shown to be temperature dependent. Even though the initial water uptake is constant for all temperatures, the specimens immersed in water at higher temperatures reach saturation faster than those at lower temperatures.

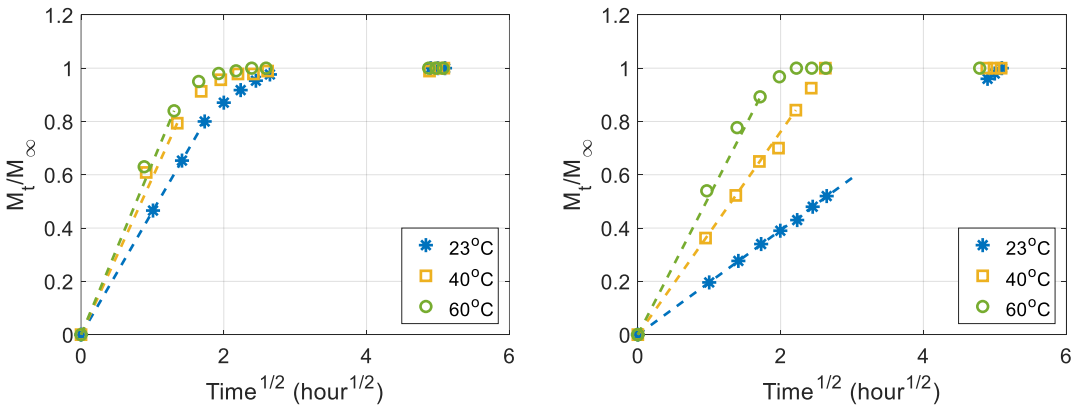

Figure 2: Average normalized mass change vs the square root of time during immersion of (a) VHB and (b) BOPP in distilled water for three different temperatures

The diffusion coefficients calculated for all three temperatures using Aminabhavi's method and Crank's method are listed in Table 1. The logarithmic values of the calculated diffusion coefficients are then plotted against the inverse of the absolute temperature as shown in Figure 3. The two methods used for the calculation of the

diffusion coefficients give similar results. The diffusion coefficients fall within 2% of each other for each respective case.

Table 1: Calculated diffusion coefficients $\left(\frac{m^2}{s}\right)$ for VHB and BOPP using either Aminabhavi's method or Crank's method

Temperature (°C)	Aminabhavi		Crank	
	VHB	BOPP	VHB	BOPP
23	7.83×10^{-12}	5.63×10^{-15}	3.91×10^{-12}	2.81×10^{-15}
45	1.13×10^{-11}	2.03×10^{-14}	5.62×10^{-12}	1.02×10^{-14}
65	2.00×10^{-11}	2.86×10^{-14}	1.00×10^{-11}	1.43×10^{-14}

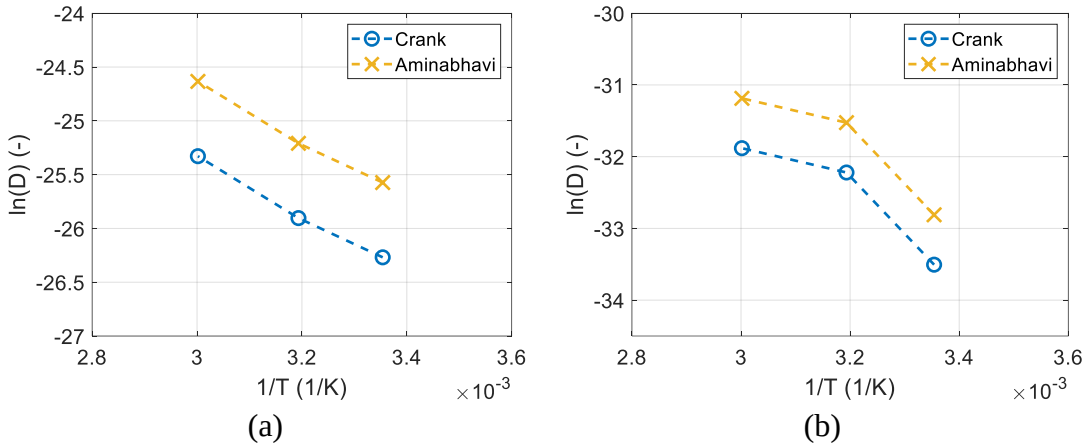

Figure 3: Determination of the activation energy for water diffusion into (a) VHB and (b) BOPP

The temperature dependence of the diffusion coefficients can be modeled using the Arrhenius equation (Equation 7) by plotting $\ln(D)$ vs $\frac{1}{T}$. The activation energy can be determined from the slope of Figure 3. Both Crank and Aminabhavi's methods produce a slope $\left(\frac{E_a}{R}\right)$of 2101.3 for VHB and 3723.2 for BOPP.

Lastly, the acceleration factor is calculated with Equation 8. Given an assumed service temperature of 17°C and an accelerated temperature of 65°C, the acceleration factor is computed to be 2.85 for VHB and 6.38 for BOPP. The difference in the acceleration factors are in alignment with the difference in thickness of the materials (i.e., the thinner material has a higher AF). Therefore, an accelerated aging period of 128 days for VHB and 57 days for BOPP is approximately 12 months of real time exposure to an underwater environment.

5 CONCLUDING REMARKS

In this paper, two commercially available dielectric elastomers, VHB4910 and BOPP, are artificially aged via accelerated life testing. An initial study of the diffusion of water into the specimens is conducted to determine the acceleration factor and the accelerated aging period given an accelerated temperature. Given a service temperature of 17°C and an accelerated temperature of 65°C, acceleration factors of 2.85 and 6.38 are determined for VHB and BOPP, respectively. This translates to accelerated aging periods of 128 and 57 days for VHB and BOPP. With these conditions, three sets of specimens can be produced: unaged specimens, and two different aged specimens at 6 months and 12 months at the service temperature. Unaged specimens provide a baseline for studied properties and a range of aged specimens show the influence of a seawater environment on these materials. The effect of aging visibly affects VHB via changes in color and stiffness. BOPP tells a different story. No visual changes are noted as aging proceeds. Future work will consist of experimental testing on the procured sets of specimens including tensile testing and dynamic mechanical analysis. These experiments will allow for a study of the changes of the material properties as the materials age. These experimental results will then be validated with a viscoelastic constitutive model. Furthermore, the influence of seawater exposure on the viscoelastic properties of the materials will be investigated via theoretical formulation, numerical modeling, and statistical validation.

6 ACKNOWLEDGEMENTS

The authors gratefully acknowledge Griff Paper and Film for the provided samples of BOPP. In addition, the authors thank Dr. Thomas Ramotowski for providing lab space and proper instrumentation needed to complete the accelerated life tests. This research has been supported by the Department of Defense SMART SEED Grant. Any opinions, findings, and conclusions or recommendations expressed in this publication are those of the authors and do not necessarily reflect the views of the funding sponsors.

7 REFERENCES

[1] Aschwanden, M. and Stemmer, A. "Low voltage, highly tunable diffraction grating based on dielectric elastomer actuators." In *The 14th International Symposium on: Smart Structures and Materials & Nondestructive Evaluation and Health Monitoring*, pages 65241N–65241N. International Society for Optics and Photonics, 2007.

[2] Aminabhavi, T.M., Thomas, R.W., and Cassidy, P.E. Predicting Water Diffusivity in Elastomers, *Polymer Engineering and Science*, 18 (1984), 1417–1420. https://onlinelibrary.wiley.com/doi/abs/10.1002/pen.760241808.

[3] Arrhenius, S.A. Über die Dissociationswärme und den Einfluß der Temperatur auf den Dissociationsgrad der Elektrolyte, *Z. Phys. Chem.*, (1889), 4:96–116. https://doi.org/10.1515%2Fzpch-1889-0408.

[4] ASTM D570-80, Standard Test Method for Water Absorption of Plastics 1, ASTM international, West Conshohocken, PA, (2019). www.astm.org
[5] ASTM D638, Standard Test Method for Tensile Properties of Plastics, ASTM International, West Conshohocken, PA, (2015). www.astm.org
[6] ASTM D882-18, Standard Test Method for Tensile Properties of Thin Plastic Sheeting, ASTM International, West Conshohocken, PA, (2018). www.astm.org
[7] Bar-Cohen, Y. and Zhang, Q. "Electroactive polymer actuators and sensors." *MRS bulletin*, 33(03):173–181, 2008.
[8] Bele, A., Stiubianu, G., Vlad, S., Tugui, C., Varganici, C.D., Matricala, L., Ionita, D., Timpu, D., and Cazacu, M. "Aging behavior of the silicone dielectric elastomers in a simulated marine environment." *RSC advances* 6, no. 11 (2016): 8941-8955.
[9] Carpi, F., De Rossi, D., Kornbluh, R., Pelrine, R., and Sommer-Larsen, P., Dielectric Elastomers as Electromechanical Transducers, Elsevier, Radarweg, Amsterdam, The Netherlands, 2007.
[10] Chenwi, I.N., Ramotowski, T., LeBlanc, J., and Shukla, A. (2021). Effects of Prolonged Saline Water Exposure on the Peel Strength of Polyurea/Monel 400 Interface. The Journal of Adhesion. http://dx.doi.org/10.1080/00218464.2021.1900829.
[11] Crank, J. The mathematics of diffusion UK: Oxford University Press, 2nd edition; (1975), ISBN-13: 978-019853411.
[12] Dehghan, M., Al-Mahaidi, R., Sbarski, I. & Gad, E. 2014. Effect of Fabrication Method on Thermo-mechanical Properties of an Epoxy Composite, The Journal of Adhesion, 90(5-6): 368-383.
[13] Heshmati, M., Haghani, R., Al-Emrani, M. Durability of CFRP/steel joints under cyclic wet-dry and freeze-thaw conditions, Composites Part B: Engineering, Volume 126, 2017, Pages 211-226, ISSN 1359-8368, https://doi.org/10.1016/j.compositesb.2017.06.011.
[14] Jung, K., Nam, J., Lee, Y., and Choi, H. "Micro inchworm robot actuated by artificial muscle actuator based on nonprestrained dielectric elastomer." In *Smart Structures and Materials*, pages 357–367. International Society for Optics and Photonics, 2004.
[15] Kennan, J.J., Peters, Y.A., Swarthout, D.E., Owen, M.J., Namkanisorn, A., Chaudhury, M.K. "Effect of saline exposure on the surface and bulk properties of medical grade silicone elastomers." *Journal of Biomedical Materials Research: An Official Journal of The Society for Biomaterials and The Japanese Society for Biomaterials* 36, no. 4 (1997): 487-497.
[16] Nash, J.L. "Biaxially oriented polypropylene film in power capacitors." *Polymer Engineering & Science* 28, no. 13 (1988): 862-870.
[17] O'Halloran, A., O'Malley, F., and McHugh, P. "A review on dielectric elastomer actuators, technology, applications, and challenges." *Journal of Applied Physics*, 104(7):9, 2008.
[18] Oldfield, D., and Symes, T. "Long term natural ageing of silicone elastomers." *Polymer testing* 15, no. 2 (1996): 115-128.

[19] Pei, Q., Rosenthal, M.A., Pelrine, R., Stanford, S., and Kornbluh, R.D. "Multifunctional electroelastomer roll actuators and their application for biomimetic walking robots." In *Smart Structures and Materials*, pages 281–290. International Society for Optics and Photonics, 2003.

[20] Pelrine, R., Kornbluh, R.D., Pei, Q., Stanford, S., Oh, S., Eckerle, J., Full, R.J., Rosenthal, M.A., and Meijer, K. "Dielectric elastomer artificial muscle actuators: toward biomimetic motion." In *SPIE's 9th Annual International Symposium on Smart Structures and Materials*, pages 126–137. International Society for Optics and Photonics, 2002.

[21] Sheng, J., Chen, H., Qiang, J., Li, B., and Wang, Y. "Thermal, mechanical, and dielectric properties of a dielectric elastomer for actuator applications." *Journal of Macromolecular Science, Part B* 51, no. 10 (2012): 2093-2104.

[22] Smith, R.C. *Smart material systems: model development*, volume 32. Siam, 2005.

[23] Stahler, D. "Types of wound film capacitors." *US Tech–The Global Electronics Publication. Arizona Capacitors Inc., Tucson, Arizona, Mid-Atlantic Tech Publications, Phoenixville, Pennsylvania, USA (Company white paper published via on-line electronics manufacturing magazine)* (2013).

[24] Streibl, M., Werner, S., Kaschta, J., Schubert, D.W., and Moos, R. "The influence of nanoparticles and their functionalization on the dielectric properties of biaxially oriented polypropylene for power capacitors." *IEEE Transactions on Dielectrics and Electrical Insulation* 27, no. 2 (2020): 468-475.